ENDOR Relaxation Study on Phenyl Substituents

M. Plato, R. Biehl, K. Möbius, and K. P. Dinse

Institut für Molekülphysik, Freie Universität Berlin

(Z. Naturforsch. **31 a**, 169–176 [1976]; received December 22, 1975)

The proton ENDOR spectra of various phenyl substituted hydrocarbon radicals in solution show a marked temperature dependence of the positions, widths, and amplitudes of particular lines. These effects are analyzed in terms of three relaxation mechanisms: (i) internal hindered rotation and (ii) torsional oscillations of the phenyl rings, and (iii) molecular tumbling. From the temperature dependence of relaxation effects caused by mechanism (i) hindrance potentials for internal rotation of phenyl rings could be determined. The results are in good agreement with the predictions of simple π-MO theory. Relaxation effects caused by (ii) turned out to be negligible. Mechanism (iii) produces strong variations in linewidths at low temperatures due to the different hyperfine anisotropies depending on nuclear position.

1. Introduction

In recent years the development of sophisticated multiple resonance methods like ENDOR (electron nuclear double resonance)[1], ELDOR (electron electron double resonance)[2], and TRIPLE (electron nuclear triple resonance)[3] has made it possible to investigate the static and dynamic behaviour of large paramagnetic systems in solution. In this paper we will be concerned with relaxation effects caused by phenyl substituents as they show up in ENDOR spectra. Phenyl substituents of radicals in solution can be involved in the following relaxation mechanisms: (i) hindered rotation, (ii) torsional oscillations, and (iii) molecular tumbling. As representatives for the phenyl substituted molecules, the anion radicals of para-terphenyl (PTP), meta-terphenyl (MTP), ortho-terphenyl (OTP), and methyl-ortho-terphenyl (MOTP) have been studied, the structural formulae of which are given in Figure 1. These molecules have been chosen because they are the simplest representatives of the class of phenyl substituted hydrocarbons which, in principle, can show all the relaxation effects mentioned above. Their static interactions have already been studied by ESR[4] and by ENDOR in this laboratory[5].

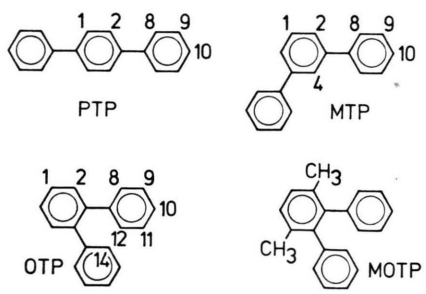

Fig. 1. Structural formulae with proton numbering of para-terphenyl (PTP), meta-terphenyl (MTP), ortho-terphenyl (OTP), and methyl-ortho-terphenyl (MOTP).

Sonderdruckanforderungen an Prof. Dr. K. Möbius, Institut für Molekülphysik am Fachbereich Physik, Freie Universität Berlin, Boltzmannstraße 20, *D-1000 Berlin 33.*

2. Experimental

The ENDOR spectrometer used has been described previously[6]. For high resolution work Zeeman modulation was omitted. Temperature variation was achieved with an AEG temperature control unit, temperature data are accurate within ± 1 K. The radicals were prepared by sodium metal reduction of the hydrocarbons in dimethoxyethane (DME) and 2-methyltetrahydrofurane (MTHF) under high vacuum conditions[7]. Radical concentrations were typically 10^{-4} moles/l to minimize exchange effects.

3. Theory

(i) Hindered Rotation

The theory adequate for describing the behaviour of ENDOR spectra affected by hindered rotation of phenyl rings has been summarized in a proceeding paper[8]. Therefore here only the final formulae are presented which were used for analyzing the spectroscopic data.

The jumping process of the two phenyl rings between different configurations for the unsymmetri-

cally substituted molecules MTP, OTP, and MOTP is strictly an example of a four jump model because the two different coupling constants of the ortho or meta protons on one ring might also depend on the particular equilibrium position of the other ring. This interaction between the two phenyl rings can, however, be neglected since, experimentally, there are only two resolved ENDOR lines for each ortho and meta group of four protons in the slow-jump limit. There is also no additional broadening on account of an unresolved splitting of these lines. In this case, we can therefore safely separate the whole process into two effectively independent two jump processes with two different splitting constants a_{I} and a_{II}.

Denoting the jumping rate by k, the additional line broadening is given by

$$1/T_2'\,(\mathrm{ENDOR}) = k \quad (\text{slow jump, } \Delta\omega_0/k \gg 1) \tag{1}$$

and

$$1/T_2'\,(\mathrm{ENDOR}) = \tfrac{1}{8}(\Delta\omega_0)^2 k^{-1} \tag{2}$$

(fast jump, $\Delta\omega_0/k \ll 1$)

where

$$\Delta\omega_0 = 2\pi \left| \frac{a_{\mathrm{I}} - a_{\mathrm{II}}}{2} \right| ,$$

the hfs constants a being measured in Hz. In the slow-jump region, k can be determined from the separation $\Delta\omega$ of the two ENDOR lines:

$$\Delta\omega^2 = \Delta\omega_0^2 - 8k^2 . \tag{3}$$

The complete range between the slow and fast jump limits can be handled by modified Bloch equations [9]. These can be used to simulate experimental spectra as a function of $\Delta\omega_0$, k and the unperturbed linewidth $1/T_2^0$. This procedure was used throughout this work.

(ii) Torsional Oscillations

Torsional oscillations of the phenyl rings can obviously modulate the anisotropic as well as the isotropic hfs interactions in the molecule. In principle, one therefore expects additional electron and nuclear relaxation. The problem is to obtain an estimate of the magnitude of the corresponding relaxation rates.

According to a semiclassical theory given by Freed and Fraenkel [10] of the effects of internal motions on ESR linewidths, a rotating substituent group (rotor) can be characterized by its moment of inertia I and a friction constant βI. The Brownian motion of the rotor is then described by the Langevin equation for the angle of rotation Θ

$$\mathrm{d}^2\Theta/\mathrm{d}t^2 + \beta\,\dot{\Theta} = A(t) + f(\Theta) , \tag{4}$$

where $A(t)$ is a random rotational acceleration describing the torques resulting from solvent collisions and $f(\Theta)\cdot I$ is a nonrandom torque acting on the rotor. For a rotor subject to a harmonic restoring torque, $f(\Theta) = -\omega_0^2(\Theta - \Theta_{\mathrm{e}})$, where $\omega_0/2\pi$ is the frequency of the oscillations and Θ_{e} is the equilibrium position. Since in our experiment the rotational barrier of phenyl rings is larger than kT by more than a factor of 10, a phenyl ring will, on the average, behave as such a harmonic oscillator (i. e. the average displacement $\overline{(\Theta - \Theta_{\mathrm{e}})^2}^{1/2}$ is small compared with $2\pi/n$, where n is the number of potential minima along a full rotation).

The modulation of the isotropic and/or anisotropic hfs interaction due to the phenyl ring oscillations can be described to first order by

$$F' = C(\Theta - \Theta_{\mathrm{e}}) \tag{5}$$

with C being constant. (The quantity F' stands for any tensor component of the spatial part of the hfs interaction energy for a particular proton in a molecule fixed axis system). As will be shown below, in our experiments the damping of phenyl rings is sufficiently large to justify the neglect of quadratic terms in $\Theta - \Theta_{\mathrm{e}}$ in Equation (5) [11]. The constant C can be of quite different magnitude for the different types of hfs interactions. In the case of the isotropic hfs interaction, C is determined solely by the variation $\Delta\varrho_{\mathrm{H}}/\Delta\Theta$ of the spin density on the 1s-H-orbital per degree of twist angle, whereas, in the case of the anisotropic hfs interaction, both the angular variation $\Delta\varrho_{\mathrm{C}}/\Delta\Theta$ of the carbon spin densities and the change in the directions of the tensor axes have to be considered. Defining the spectral density function, as usual, by

$$j(\omega) = \tfrac{1}{2}\int_{-\infty}^{+\infty} \overline{F'(t)\,F'(t+\tau)}\, e^{-i\omega\tau}\,\mathrm{d}\tau \tag{6}$$

one obtains directly from Eqs. (4) and (5) [12]

$$j_{\mathrm{osc}}(\omega) = C^2\,\overline{(\Theta - \Theta_{\mathrm{e}})^2}\,\beta\,\omega_0^2\,[(\omega^2 - \omega_0^2)^2 + \beta^2\omega^2]^{-1} . \tag{7}$$

The time average of $(\Theta - \Theta_{\mathrm{e}})^2$ is given by the relation [10]

$$\overline{(\Theta - \Theta_{\mathrm{e}})^2} = kT/(I\,\omega_0^2) . \tag{8}$$

The spectral density function in Eq. (7) has the same frequency dependence as the square of the amplitude of a harmonic oscillator with resonant frequency ω_0 which is driven by a periodic force $F_0 \cos \omega t$. This implies that for small dampings $\beta \ll \omega_0$ large spectral densities will be mainly found close to ω_0. For larger dampings $\beta > \omega_0$ the maximum of $j(\omega)$ is shifted towards $\omega = 0$ and, finally, for $\beta \gg \omega_0$, $j_{osc}(\omega)$ approaches the functional form $\tau_{osc}(1+\tau_{osc}^2 \omega^2)^{-1}$ with $\tau_{osc} = \beta/\omega_0^2$.

While from our experiments (vide infra) ω_0 is known to be in the order of $10^{13}\ s^{-1}$, the constant β has to be estimated theoretically. This is done on the basis of a crude model. If the shape of the rotor approximates that of a sphere, β is given macroscopically by [10] $\beta = 8\pi\eta a^3/I$ where a is the radius of the sphere and η is the viscosity of the solvent. Taking the effective radius of a phenyl ring to be 2 Å and calculating I from well known bond lengths and atomic masses ($I = 1.5 \times 10^{-38}$ g cm^2) one obtains $\beta \approx 5 \times 10^{14}\ s^{-1}$ for DME at 190 K ($\eta = 3$ cP). We therefore have the case of extremely large damping, where $j_{osc}(\omega)$ can be represented by

$$j_{osc}(\omega) = C^2 \overline{(\Theta - \Theta_e)^2}\, \tau_{osc}(1+\tau_{osc}^2 \omega^2)^{-1}$$
with $\tau_{osc} = \beta/\omega_0^2$. (9)

For DME at 190 K one therefore obtains $\tau_{osc} \approx 5 \times 10^{-12}$ s. This value is considerably shorter than the rotational correlation time $\tau_R \approx 10^{-9} \ldots 10^{-10}$ s of molecules like para-terphenyl at the same temperature (see Section 4). Since the spectral density at $\omega = \omega_{NMR} \ll \tau_R^{-1}$ due to rotational motion is given by [13]

$$j_{rot}(\omega_{NMR}) = \text{Trace}\,(A^2)\tau_R/5 \qquad (10)$$

where A is the anisotropic hfs tensor of the observed proton, additional nuclear spin lattice relaxation (W_n) from torsional oscillations will, therefore, not be safely detectable unless $C^2 \overline{(\Theta - \Theta_e)^2}$ exceeds $\text{Tr}(A^2)$ by at least a factor of 10. From Eq. (8) we have $\overline{(\Theta - \Theta_e)^2} \approx 2 \times 10^{-2}$ rad^2 at $T = 190$ K. Taking 2 MHz^2 as the minimum value of $\text{Tr}(A^2)$ found in the terphenyl radicals, the constant C in Eq. (5) would therefore have to be in the order of 30 MHz. This can certainly not be achieved in the terphenyls where all isotropic and anisotropic hfs couplings themselves are considerably smaller than 30 MHz. Cross relaxation effects caused by torsional oscillations are also not expected to be observable in the ENDOR spectra because they cannot compete with the very much larger nuclear relaxation rate W_n caused by molecular tumbling. The same argument holds for secular T_2-effects of the oscillatory motion. As will be shown in the following section, the ENDOR linewidth is at least in the order of the nuclear relaxation rate caused by molecular tumbling. We therefore conclude that relaxation effects caused by torsional oscillations can be neglected compared with those by molecular tumbling.

(iii) Molecular Tumbling

Molecular tumbling in solution caused by collisions with the solvent molecules can produce various kinds of nuclear and electron relaxation processes [14]. The most important relaxation mechanism in ENDOR studies on hydrocarbon radicals in solution is the modulation of the electron-nuclear dipolar (END) interaction giving rise to pure electron relaxation (rate W_e), pure nuclear relaxation (W_n), and cross relaxation (W_x). The dependence of the ENDOR signal amplitudes on these various relaxation rates are treated in a series of papers by Freed [15]. Here we will be mainly concerned with the question of how (unsaturated) ENDOR linewidths depend on the END mechanism and on temperature. Particularly at low temperatures (e. g. $T \approx 200$ K in DME), pronounced variations in the unsaturated linewidth turned out to be the main cause for the observed differences in ENDOR amplitudes of different protons.

In the single line approximation [16], the transverse relaxation rate T_{2n}^{-1} of a nuclear transition a $\longleftrightarrow$ b is given by

$$T_{2n}^{-1} = T_{2n}'^{-1} + (t_a^{-1} + t_b^{-1})/2\,. \qquad (11)$$

In this equation $T_{2n}'^{-1}$ describes the broadening due to modulation of the secular terms of the spin Hamiltonian and t_a and t_b are the lifetimes of the states a and b. These lifetimes are determined by the sums of the relaxation rates connecting a and b to the various other states of the system [16]:

$$t_i^{-1} = \sum_{j \neq i} W_{ij}\,, \quad i = a, b\,. \qquad (12)$$

Taking the simplest system of one electron and one proton and neglecting cross relaxation rates we have $t_a = t_b = (W_e + W_n)^{-1}$. Since for NMR in solution (fast tumbling limit) $T'_{2n} \approx 2\,T_{1n} = W_n^{-1}$ we can write

$$T_{2n}^{-1} = W_e + 2\,W_n\,. \qquad (13)$$

In the temperature region where ENDOR in solution is normally performed, $\omega_e \tau_R \gg 1$ and $\omega_n \tau_R$

$\ll 1$, where τ_R is the rotational correlation time. Since the spectral density is proportional to $\tau_R/(1+\omega^2\tau_R^2)$, this implies $W_e \propto \tau_R^{-1}$ and $W_n \propto \tau_R$ thus giving

$$T_{2n}^{-1} = A\,\tau_R^{-1} + B\,\tau_R \qquad (14)$$

with constants A and B solely determined by the magnitude of the various intramolecular magnetic interactions. Considering the strong temperature dependence of τ_R, T_{2n}^{-1} will either decrease or increase with varying temperature depending critically on the relative magnitude of W_e and W_n. The minimum linewidth is encountered at a temperature corresponding to the correlation time $\tau_R = (A/B)^{1/2}$. Since W_e is mainly determined by g-factor anisotropy and spin-rotational interaction [17], the constant A is practically independent of the nuclear position in the molecule. The constant B, on the other hand, can be very different for different nuclei depending on the magnitude of the hfs anisotropy. From [13] $W_n = \frac{1}{2} j_{rot}(0)$ and Eqs. (13) and (14) one obtains

$$B = \tfrac{1}{5}\,\mathrm{Tr}\,(A^2)\,. \qquad (15)$$

It is thus predicted, that – provided W_n and W_e become comparable anywhere in the studied temperature range – there will be an increasing dependence of the linewidth on the nuclear position towards lower temperatures. This dependence shows up in such a way that lines belonging to nuclei with the larger values of $\mathrm{Tr}(A^2)$ will broaden sooner.

4. Results and Discussion

The ESR spectra of OTP and MTP change strongly with temperature. For OTP this is demonstrated in Figure 2. No such temperature dependence has been observed for PTP. While an analysis of these spectra is almost hopeless, from the ENDOR spectra (Fig. 3) one immediately sees that only particular coupling constants change significantly with temperature. A closer look at the spectrum in Fig. 3 reveals two pairs of coupling constants showing a temperature behaviour typical for nuclear spins jumping between inequivalent magnetic sites [18].

By simulation of the experimental ENDOR spectra on the basis of modified Bloch equations we obtained the rate constant k as a function of temperature. The unperturbed linewidths required for this procedure at the various temperatures were taken from a line not involved in the jump process. Since in ENDOR experiments all lines show a considerable saturation broadening, all linewidths were extrapolated to zero NMR power.

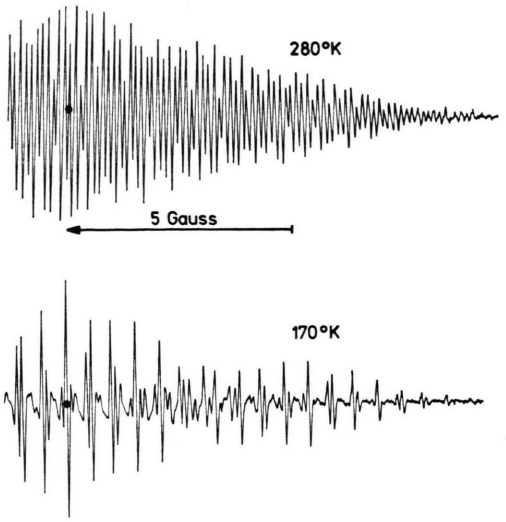

Fig. 2. ESR spectrum of OTP at different temperatures.

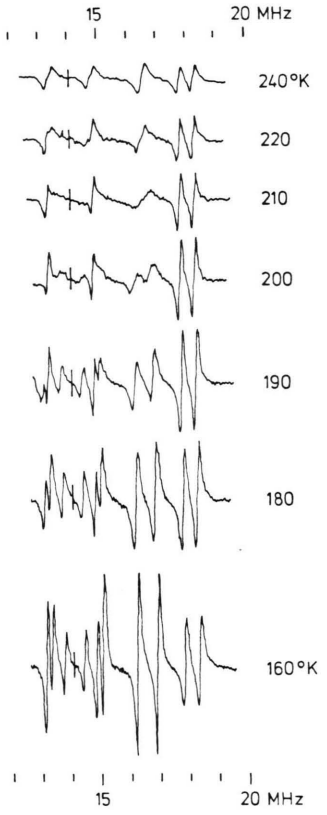

Fig. 3. ENDOR spectrum of OTP at different temperatures.

Figure 4 shows the Arrhenius plots of $k = k(T)$ for OTP, MTP, and MOTP. The linearity of the

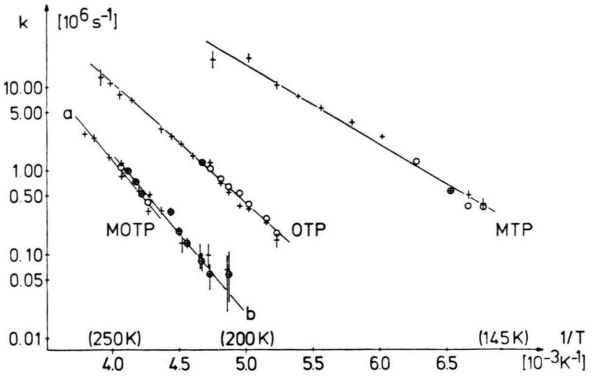

Fig. 4. Arrhenius diagrams of the phenyl jumping rate constants $k=k(T)$ for OTP, MTP, and MOTP. The crosses and circles were derived from measurements of ENDOR linewidths [Eqs. (1) and (2)] and line separations [Eq. (3)], respectively.

plots shows that we are dealing with a thermally activated process describable by $k=k_0\cdot\exp\{-E_a/kT\}$. For MOTP it was possible to evaluate the temperature dependence for both the ortho- and meta-protons (lines a and b in Figure 4). The results are equal within the experimental error. The activation energies E_a and preexponential factors k_0 are collected in Table 1.

Table 1. Activation energies and preexponential factors for hindered rotation of phenyl rings (1 eV=23.04 kcal mole^{-1}).

	E_a [eV]	k_0 [s^{-1}]
OTP	0.286±3%	$6\times10^{(12\pm.5)}$
MTP	0.187±4%	$1\times10^{(12\pm.5)}$
MOTP	0.394±3%	$1\times10^{(14\pm.5)}$

We attribute the observed jump process to hindered rotation of the phenyl rings for the following reasons:

The isotropic hfs couplings reflecting the jump process occur in two pairs in each molecule. In the high temperature limit each pair collapses into one line belonging to 4 equivalent protons as has been proven by simulating the ESR spectrum with the ENDOR data. Those protons can only be assigned to the phenyl rings since there is no accidental degeneracy of hfs couplings.

This conclusion is consistent with the result that in MOTP both pairs of ENDOR lines yield the same E_a and k_0.

Using the simple mechanical model proposed by Das [19], we interpret the measured E_a values as the molecular potential barrier V_h for hindered rotation of the phenyl rings. In this same model k_0 corresponds to twice the frequency of the corresponding harmonic oscillator. The application of this model is somewhat problematic because any contributions to E_a from changes in the solvation shell during a phenyl jump are excluded. These contributions are possibly of considerable magnitude because for the pure solvent DME the activation energy taken from the viscosity temperature dependence is as high as 0.08 eV [20]. This activation energy is rather similar for other suitable solvents so that these contributions to E_a cannot be detected experimentally just by changing the solvents. On the other hand, our interpreteation of E_a as an intramolecular quantity is consistent with MO calculations, as will be shown subsequently. We therefore assume

$$E_a = V_h \tag{16}$$

where V_h is defined as the difference between the maximum total energy of the molecule and the total energy for the equilibrium positions of the phenyl rings.

MO calculations of potential barriers have been performed in the frame of the simple HMO model, where

$$V_h = E_\pi(90°) - E_\pi(\Theta_e)\,. \tag{17}$$

The effective resonance integral $\beta=-0.78$ eV was taken from the literature [21]. We have refrained from using more advanced MO methods like CNDO or INDO since these methods generally do not give improved results in this respect [22].

Figure 5 shows the dependence of V_h on Θ_e for OTP and MTP. For OTP we assumed a correlated jump of the two phenyl rings because of extreme steric hindrance. This is obvious from molecular

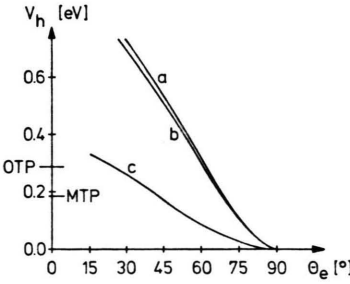

Fig. 5. Calculated molecular potential barrier for hindered phenyl rotation in OTP (curve a) and MTP (curves b and c) as a function of equilibrium angle. Curve b is for a fully correlated jump, curve c for a noncorrelated jump of the two phenyl rings in MTP (see text). The experimental values of V_h for OTP and MTP are marked on the V_h axis.

models which show that the two phenyl rings are interlocked. For MTP, on the other hand, the following possibilities have been considered:

(i) a fully correlated jump,
(ii) a noncorrelated jump.

They differ considerably in their dependence of V_h on Θ_e. The comparison with the experimentally observed V_h values gives $\Theta_e = 65°$ for OTP. For MTP one obtains $\Theta_e = 70°$ for case (i) and $\Theta_e = 40°$ for case (ii). The value of Θ_e for OTP appears reasonable on account of space filling molecular models and hfs calculations [4, 5]. From the same arguments for MTP case (i) is rejected and we are left with an uncorrelated jumping of the phenyl rings.

The MOTP shows a surprisingly high E_a in view of the fact that the methyl groups are not expected to change the equilibrium angle compared with OTP since the phenyl rings are already highly twisted. Furthermose, if there were an increase in the twist angle, this should result in an even smaller potential barrier. Since the terphenyl anions have non-degenerate ground states and methyl groups are known to be weak substituents in this case, one also does not expect a significant change in $V_h(\Theta)$ as compared with OTP. This is supported by MO calculations using both the hetero atom and hyperconjugative model [23] for the methyl substituent. Given the limitations of simple π-MO frame-work we can reproduce the larger value of V_h for MOTP by introducing a weak bonding $\beta/\beta_0 = 0.4$ for $\Theta_e = 60°$ between the methyl group and the nearest C atoms of the phenyl rings. It is important to point out, that the introduction of this additional bonding does not alter the spin density distribution significantly, which is still in good agreement with the ENDOR results.

As can be seen from Fig. 3 the ENDOR lines of the phenyl ortho and meta protons show a remarkable increase in amplitude towards lower temperatures in comparison with the remaining protons. We have observed the same also for other phenyl substituted radicals [24]. This effect becomes particularly pronounced in the temperature region where relaxation from hindered rotation is no longer observable. Furthermore, this effect is also observed for para terphenyl where for symmetry reasons relaxation through hindered rotation is absent.

As was shown in Sect. 3 (ii), for the terphenyl anions torsional oscillations do not contribute significantly to this effect. We are therefore left with the possibility that the various protons involved might have significantly different hfs anisotropies. This can lead to contributions both to W_n and T_{2n}^{-1}. The ENDOR signal amplitude E for differential fm modulation and phase sensitive detection is given by

$$E \propto \frac{d_n^2 T_{2n}^2}{(1 + 4 d_n^2 T_{2n} T_{1n\,\mathrm{eff}})^{3/2}} \qquad (18)$$

where $d_n = \frac{1}{2}\gamma_n B_n$ and the induced transition rate $d_n^2 T_{2n}$ is proportional to the NMR power. If measurements are performed in the low NMR saturation limit, where $4 d_n^2 T_{2n} T_{1n\,\mathrm{eff}} \ll 1$, E is independent of $T_{1n\,\mathrm{eff}}$ and proportional to the inverse square of the linewidth T_{2n}^{-1} provided the NMR field is kept constant over the spectrum range. For saturation parameters $4 d_n^2 T_{2n} T_{1n\,\mathrm{eff}} \gtrsim 1$ the dependence of E on T_{2n} is less pronounced but E will still increase with decreasing linewidth T_{2n}^{-1}. We therefore conclude that the different temperature dependences of the various ENDOR line amplitudes result from different temperature dependences of T_{2n}^{-1}. A constant NMR field has been experimentally assured.

In order to test this conclusion, calculations of electron nuclear dipolar tensors according to the method of McConnell-Strathdee [25] and Derbyshire [26] were performed. As results of these calculations the values for the squares of the anisotropies $\mathrm{Tr}(A^2)$ for PTP are given in Table 2.

The next step is to calculate the temperature dependence of T_{2n}^{-1}. For this purpose one has to

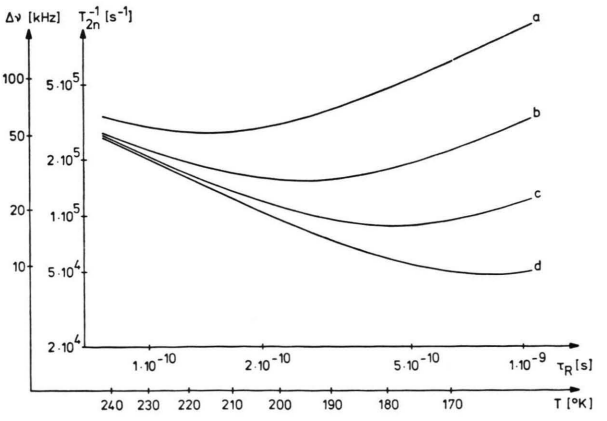

Fig. 6. Theoretical ENDOR linewidth as a function of the rotational correlation time and temperature (for PTP in DME) for different hfs anisotropies $\mathrm{Tr}(A^2) = 100\ \mathrm{MHz}^2$ (a), $30\ \mathrm{MHz}^2$ (b), $10\ \mathrm{MHz}^2$ (c), $3\ \mathrm{MHz}^2$ (d). A Lorentzian line shape has been assumed.

Table 2. Calculated anisotropies for the protons of PTP(−).

position	$\mathrm{Tr}(A^2)$ [MHz²]
8 (ortho phenyl)	19
9 (metha phenyl)	2.3
10 (para phenyl)	57
1,2 (central ring)	15

determine the quantities A and B in Equation (14). A, being independent of nuclear spin quantum numbers, was determined from the ENDOR linewidth at a high temperature (240 K) where $T_{2n}^{-1} = A/\tau_R$. The correlation time τ_R at this temperature was estimated from the well-known relation $\tau_R = 4\pi\eta r^3/3kT$ which gives $\tau_R = 8\cdot10^{-11}$ s using $\bar{r} = 4$ Å and $\eta(240\,\mathrm{K}) = 1$ cP (DME [20]). From the measured linewidth $\Delta\nu_n = (\pi\sqrt{3}\,T_{2n})^{-1} = 50$ kHz we obtain $A \approx 2\cdot10^{-5}$. Using Eq. (15) we finally have

$$T_{2n}^{-1} \approx 2\cdot10^{-5}/\tau_R + \mathrm{Tr}(A^2)\cdot10^{13}\,\tau_R \qquad (19)$$

when $\mathrm{Tr}(A^2)$ is measured in MHz².

Equation (19) has to be looked at as a rather crude approximation to the true ENDOR linewidths in the terphenyl radical anion, since in contrast to the theoretical assumptions, (i) there is more than one proton contributing to any phenyl proton ENDOR line, and (ii) chemical exchange might also contribute to the experimental linewidths. The latter effect, however, is not expected to depend on nuclear positions whereas the former can only change the numbers in Eq. (19) by factors in the order of 1 which is unimportant in view of the large uncertainty in the calculation of τ_R. The dependence of T_{2n}^{-1} on τ_R for different anisotropies is plotted in Figure 6. This plot demonstrates that for anisotropies in the order of 10 MHz² both contributions to T_{2n}^{1} in Eq. (14) are of comparable magnitude in a low temperature region still accessible for ENDOR in solution work.

Inserting the actual anisotropies for the PTP protons given in Table 2, the temperature dependences of the various linewidths were calculated (see Figure 7). Also shown in Fig. 7 are the experimental ENDOR linewidths.

The experimental linewidth of the para protons increases by a factor of two when the temperature desreases from about 220 to 180 K. This is accompanied by an apparent decrease of the amplitude by a factor of four when keeping the fm deviation constant. For the para protons these observations are in

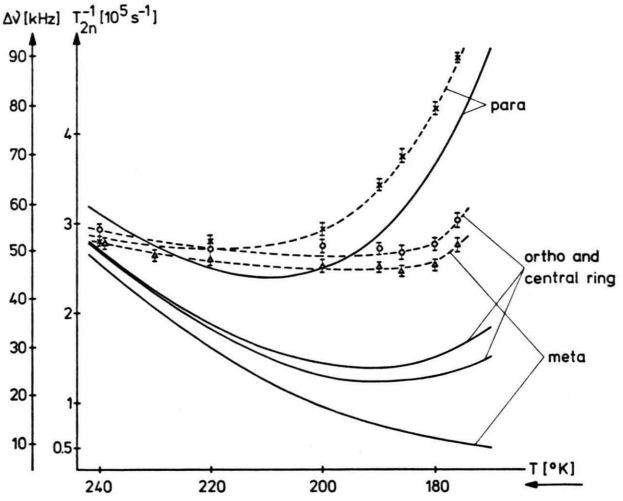

Fig. 7. Theoretical (solid lines) and experimental (dotted lines) ENDOR linewidths for different protons in PTP as a function of temperature. Solvent: DME.

sufficiently good agreement with the theory to support our assumption that modulation of the END interaction by molecular tumbling is the main cause of linewidth and amplitude variations in the ENDOR spectra. The ortho-, meta- and central ring proton lines, on the other hand, show a less satisfactory agreement with the theory. The reason for this is found in a residual linewidth of about 40 kHz which is larger than the calculated END contribution at temperatures below 200 K. This residual linewidth cannot be attributed to fm modulation broadening or second order splittings. From the work of Freed et al. [28] it is known that the microwave field H_1 produces a coherence splitting of the ENDOR lines which for $\gamma_e H_1 \gg 1/T_{2e}$, $1/T_x$, $1/T_{2n}$ is given by $(\gamma_e/2\pi)H_1$. In the intermediate region the splitting or apparent line broadening due to this effect can be calculated only when all the relaxation times of the system are known. Since ENDOR experiments always require at least partly saturating microwave fields for sensitivity reasons, it was not possible to reduce $(\gamma_e/2\pi)H_1$ below approximately (50 ± 20) kHz. The corresponding microwave power was then already 16 db below the optimum value for the maximum ENDOR signal. An extrapolation to the unperturbed NMR linewidth was not possible because the linebroadening is an unknown function of H_1. However, under the prevailing conditions of extremely high resolution (ESR linewidth = 18 ± 2 mG, pumping a single resolved ESR line with-

out Zeeman modulation), we were still able to observe a coherence splitting of the meta, ortho, and ring proton ENDOR lines for $(\gamma_e/2\pi)H_1 \approx 50$ kHz at $T \approx 200$ K. By fitting the observed lineshape with two superimposed Lorentzian lines we were able to obtain an upper limit of (15 ± 5) kHz for the unperturbed ENDOR linewidth. This value is consistent with the linewidth calculated for pure END interaction at the same temperature. No coherence splitting of this kind was obtained for the para protons because of the larger unperturbed ENDOR linewidth.

5. Conclusion

In conclusion we can state that mechanism (iii), i. e. molecular tumbling, gives an adequate explanation for the observed different temperature dependences of ENDOR lines in the low temperature region where hindered rotation no longer contributes to ENDOR relaxation. This implies that mechanism (ii), i. e. torsional oscillations of phenyl groups, does not play a dominant role as was expected from theoretical reasoning. We can furthermore deduce the following general behaviour of phenyl proton ENDOR lines:

Since the meta protons will generally have the smallest hfs anisotropy, their ENDOR lines will be the last ones to disappear when cooling down the sample. The contrary is true for the para protons which on account of their large anisotropy will disappear already at moderately low temperatures. This holds, provided the spectra are not recorded in the high NMR saturation limit, since for high saturation the temperature dependence of the ENDOR enhancement is dominated by W_n which has the same temperature dependence for all protons. These different temperature dependences at low NMR power levels can be exploited as an aid for assignment purposes, particularly when hindered rotation cannot be observed due to the symmetry of the moleceule. This effect is in close resemblance to the temperature dependence of rotating methyl groups which has also been used for assignment purposes [27].

Acknowledgements

This work was supported by the Deutsche Forschungsgemeinschaft (SFB 161). It is a pleasure to acknowledge many helpful discussions with C. von Borczyskowski about relaxation effects of phenyl substituents. We want to thank Prof. Dr. E. de Boer, University of Nijmegen, for supplying us with a computer program for hfs tensor calculations.

[1] K. Möbius and K. P. Dinse, Chimia **26**, 461 [1972].
[2] K. H. Hausser and D. Stehlick, Advances in Magnetic Resonance, Vol. III, New York, Acad. Press 1968.
[3] K. P. Dinse, R. Biehl, and K. Möbius, J. Chem. Phys. **61**, 4335 [1974].
[4] K. H. Hausser, L. Mongini, and R. von Steenwinkel, Z. Naturforsch. **19 a**, 777 [1963].
[5] R. Biehl, K. P. Dinse, and K. Möbius, Chem. Phys. Lett. **10**, 605 [1971].
[6] K. P. Dinse, K. Möbius, and R. Biehl, Z. Naturforsch. **28 a**, 1069 [1973].
[7] K. Scheffler and B. H. Stegman, Elektronenspinresonanz, Springer-Verlag, Berlin 1970.
[8] C. von Borczyskowski, K. Möbius, and M. Plato, J. Magn. Res. **17**, 202 [1975].
[9] H. S. Gutowsky, D. M. McCall, and C. P. Slichter, J. Chem. Phys. **21**, 279 [1953].
[10] J. H. Freed and G. K. Fraenkel, J. Chem. Phys. **41**, 3623 [1964].
[11] A. Abragam, The Principles of Nuclear Magnetism, Oxford Univ. Press, London and New York 1961, Chapter X, Section VI, A.
[12] S. O. Rice, Bell System Tech. J. **23**, 282 [1944].
[13] J. H. Freed, in: Electron Spin Relaxation in Liquids, ed. L. T. Muus and P. W. Atkins, Plenum Press, New York 1972.
[14] J. H. Freed and G. K. Fraenkel, J. Chem. Phys. **39**, 326 [1963].
[15] J. H. Freed, J. Chem. Phys. **43**, 2312 [1965].
[16] A. Abragam, The Principles of Nuclear Magnetism, Oxford Univ. Press, London 1961, Chapter X, Section III, B.
[17] D. S. Leniart, H. D. Connor, and J. H. Freed, J. Chem. Phys. **63**, 165 [1975].
[18] A. Carrington and A. D. McLachlan, Introduction to Magnetic Resonance, Harper & Row, New York 1969, Section 12.2.
[19] T. P. Das, J. Chem. Phys. **27**, 767 [1957].
[20] Landolt-Börnstein, Zahlenwerte und Funktionen, Vol. II, Springer-Verlag, Berlin 1969.
[21] W. Kaminski and K. Möbius, Z. Naturforsch. **25 a**, 635 [1970].
[22] B. Tinland, Theor. Chim. Acta Berlin **11**, 452 [1968].
[23] A. Streitwieser, Jr., Molecular Orbital Theory, John Wiley & Sons, New York 1961.
[24] C. von Borczyskowski and K. Möbius, Chem. Phys., to be published.
[25] H. M. McConnell and T. Strathdee, Mol. Phys. **2**, 129 [1959].
[26] W. Derbyshire, Mol. Phys. **5**, 225 [1962].
[27] K. Möbius, H. van Willigen, and A. H. Maki, Mol. Phys. **20**, 289 [1971].
[28] J. H. Freed, D. S. Leniart, and J. S. Hyde, J. Chem. Phys. **47**, 2762 [1967].